Raman scattering from misfit layer compounds $(RS)_xTaS_2$ (R identical to La,Ce,Sm or Gd; S identical to sulphur; x approximately=1.2)

1995 J. Phys.: Condens. Matter 7 5383

(http://iopscience.iop.org/0953-8984/7/27/023)

J. Phys.: Condens. Matter 7 (1995) 5383–5393. Printed in the UK

Raman scattering from misfit layer compounds $(RS)_xTaS_2$ (R ≡ La, Ce, Sm or Gd; S ≡ sulphur; $x \simeq 1.2$)

K Kisoda†, M Hangyo‡, S Nakashima†, K Suzuki§¶, T Enoki§ and Y Ohno‖

† Department of Applied Physics, Osaka University, 2-1 Yamadaoka, Suita, Osaka 565, Japan
‡ Research Center for Superconducting Materials and Electronics, Osaka University, 2-1 Yamadaoka, Suita, Osaka 565, Japan
§ Department of Chemistry, Tokyo Institute of Technology, Ookayama, Meguro-ku, Tokyo 152, Japan
‖ Department of Physics, Utsunomiya University, 350 Mine-machi, Utsunomiya 321, Japan

Received 9 February 1995

Abstract. Polarized Raman scattering experiments on misfit layer compounds $(RS)_xTaS_2$ (R ≡ La, Ce, Sm or Gd; S ≡ sulphur; $x \simeq 1.2$) have been carried out in order to investigate the effect of the charge transfer (CT) from an RS layer to a TaS_2 layer on the vibrational motion. The mode assignment is made by comparing the spectra of $(RS)_xTaS_2$ with those of 2H-TaS_2 and $(RS)_xNbS_2$. The modes at frequencies below about 200 cm^{-1} are ascribed to the intralayer modes of the RS layer and the main peaks higher than 200 cm^{-1} are ascribed to the intralayer modes of the TaS_2 layer. The E mode relevant to the TaS_2 layer shifts upwards by about 40 cm^{-1} relative to the corresponding mode in 2H-TaS_2 while the A mode hardly shifts. In addition to the intralayer modes of each layer, extra modes which show an anisotropy in the basal plane are observed at 360–370 cm^{-1}. These observations indicate that the restoring forces for intralayer and interlayer interactions strengthen owing to the CT. The two-phonon Raman band is observed at higher frequencies than that of 2H-TaS_2. The comparison with the spectra of $(RS)_xNbS_2$ shows that the amount of the CT in $(RS)_xTaS_2$ is less than that in $(RS)_xNbS_2$.

1. Introduction

Misfit layer compounds $(RS)_xTaS_2$ (R ≡ rare-earth elements; S ≡ sulphur; $x \simeq 1.2$), designated as $RTaS_3$ here, consist of the alternate stacking of RS and TaS_2 layers along the c axis. The RS layer is arranged as the rocksalt type with R and S atoms, but slightly distorted in such a way that the R atoms protrude into the adjacent TaS_2 layers. On the other hand, the TaS_2 layer almost preserves the 2H-TaS_2 coordination.

The $RTaS_3$ compounds have been studied by various experimental techniques such as electrical resistivity [1–5], Hall effect [2,4], Seebeck effect [1,4,5], magnetoresistance [1,3,4], magnetic susceptibility [1,3,5], magnetization [1,3], optical reflectance [2], specific heat [1] and x-ray photoemission spectroscopy [4] measurements.

$RTaS_3$ can be regarded as an intercalation compound of the parent compound 2H-TaS_2. Many of the intercalation compounds are stabilized by the charge transfer (CT) from guest atoms or molecules to host layers. In $RTaS_3$, the charges (electrons) of the RS layer move into the d band of the Ta atom in the TaS_2 layer. We have reported previously that in $RNbS_3$ the CT affects the frequencies of the intralayer vibrational modes of the NbS_2 layer and the

¶ Present address: Institute of Physics and Chemistry, Yokohama National University, 156 Tokiwadai, Hodogaya-ku, Yokohama 240, Japan.

0953-8984/95/275383+11$19.50

strong interlayer interaction caused by the CT breaks the pseudo-hexagonal symmetry of the NbS_2 layer [6]. Similar effects are expected for $RTaS_3$, since $RTaS_3$ has essentially the same crystal structure as $RNbS_3$ and the electronic band structures may also be similar to each other. However, some differences should exist for the electronic band structure or the electron–phonon interaction between the host compounds 2H-TaS_2 and 2H-NbS_2 because the former compound undergoes the normal–incommensurate charge-density-wave (CDW) transition at 75 K with decreasing temperature whereas the latter does not. From this point of view, it is interesting to compare the vibrational spectra of $RTaS_3$ with those of $RNbS_3$.

Strong two-phonon bands have been observed in the Raman spectra of the 2H-polytype transition-metal dichalcogenides in the normal phase [7]. These strong two-phonon bands are closely related to the Kohn anomaly of the acoustic phonon induced by the nesting of the quasi-two-dimensional Fermi surface. It is expected that the CT affects the two-phonon band in $RTaS_3$ through the change in the nesting.

In this paper, the vibrational properties of $RTaS_3$ have been studied by Raman scattering spectroscopy. The results obtained in this study are compared with those of pristine compound 2H-TaS_2, ethylenediamine (EDA)-intercalated TaS_2 and the isostructural compounds $MNbS_3$ (M ≡ Sn or Pb) and $RNbS_3$ (R ≡ La or Ce). The E mode (in-plane vibrations of Ta and S atoms) in the TaS_2 layer shifts upwards relative to the E^1_{2g} mode of 2H-TaS_2. In contrast with the E mode, the frequency of the A mode (out-of-plane vibrations of S atoms) in the TaS_2 layer is nearly the same as the A_{1g} mode of 2H-TaS_2. The amount of upshift in the E mode is comparable with that of $RNbS_3$ [6] and considerably larger than that of EDA-intercalated TaS_2 [8] and Sn(or Pb)NbS_3 [9]. In addition to these bands, the bands which cannot be attributed to the intralayer vibration of the isolated TaS_2 or RS layer are observed and show anisotropy in the basal (a–b) plane similarly to the spectra of $RNbS_3$ [6]. Two-phonon Raman bands are seen for $RTaS_3$, the energy of which is higher than that of 2H-TaS_2. These vibrational characteristics are discussed in relation to the CT.

2. Experimental details

Single crystals were grown by a chemical vapour transport method using iodine as the transport agent. A mixture of the source elements was sealed in an evacuated quartz tube and heated in a two-zone furnace with a temperature gradient of 950–850 °C for 1 or 2 weeks. A typical size of the crystals used in the present experiment was 5 mm × 5 mm × 0.01 mm. The details of the crystal growth have been described elsewhere [4].

Raman scattering measurements were carried out using the a–b plane of the crystal in the quasi-back-scattering geometry at room temperature and 40 K. The sample was cleaved with adhesive tape just before the measurement. The scattered light was dispersed by a Spex 1403 double monochromator equipped with a liquid-nitrogen-cooled charge-coupled device (CCD) detector or a photomultiplier. The 4880 or 5145 Å line of an Ar^+ ion laser was used for excitation.

3. Results and discussion

3.1. Raman spectra of $RTaS_3$

Unpolarized Raman spectra of $RTaS_3$ (R ≡ La, Ce, Sm or Gd) measured at room temperature are shown in figure 1. The spectra of the four misfit layer compounds are similar because they have essentially the same crystal structure. (The stacking of the layers is somewhat

different for the four compounds, i.e. the RS sublattice contains one RS layer in the unit cell for $LaTaS_3$ and $CeTaS_3$ whereas it contains two RS layers for $SmTaS_3$ and $GdTaS_3$ [10].) For each spectrum, six or seven bands are observed. The peak frequency of the lowest band (about 120 cm^{-1}) in each spectrum decreases from about 122 cm^{-1} (La) to 116 cm^{-1} (Gd) on replacing La by heavier atoms. The frequency of the second-lowest band (about 150 cm^{-1}) shows no appreciable dependence on the rare-earth metals. Bands in the frequency region from 200 to 300 cm^{-1} have a complex structure (having at least two peaks). A pair of bands are commonly observed at about 325 and about 400 cm^{-1}. In addition to these bands, a band at around 357 cm^{-1} is observed for $LaTaS_3$ and $CeTaS_3$. This band is weak for $SmTaS_3$ and $GdTaS_3$. We have measured polarized Raman spectra at room temperature in order to assign the Raman bands. Figure 2 shows the polarized Raman spectra of $RTaS_3$ (R ≡ La, Ce or Gd). The sharp band at about 325 cm^{-1} remains Raman active in cross polarization geometry ($c(ab)\bar{c}$) for each spectrum. The Raman spectra of 2H-TaS_2 are shown in figure 3 for comparison. The spectra of 2H-TaS_2 are essentially the same as those reported previously [8, 11, 12]. The bands at about 190, about 286 and about 400 cm^{-1} are the two-phonon band, the E^1_{2g} mode and the A_{1g} mode, respectively. Table 1 summarizes the peak frequencies of all the measured peaks as well as those of 2H-TaS_2 and EDA-intercalated TaS_2 [8]. We assume that all observed bands in each spectrum of $RTaS_3$ consist of the bands related to the RS layers and the TaS_2 layers, two-phonon Raman bands, and a band that cannot be attributed to the RS and TaS_2 layers.

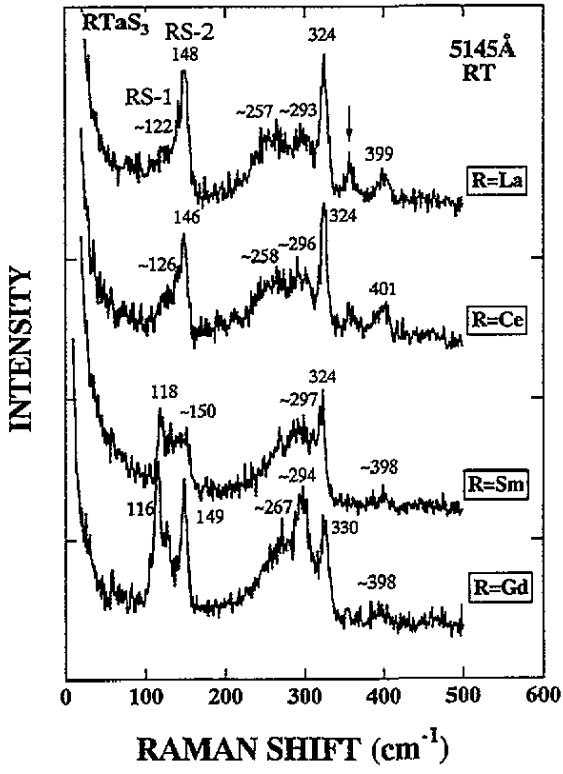

Figure 1. Unpolarized Raman spectra of $RTaS_3$ (R ≡ La, Ce, Sm or Gd) measured at room temperature.

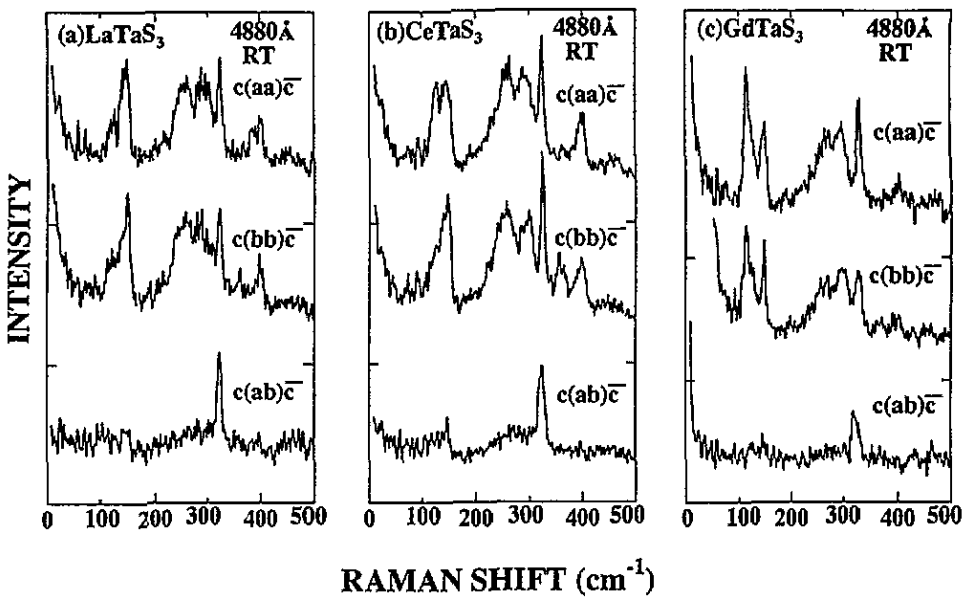

Figure 2. Polarized Raman spectra of $RTaS_3$ (R ≡ La, Ce or Gd) measured at room temperature with the three scattering configurations $c(aa)\bar{c}$, $c(bb)\bar{c}$ and $c(ab)\bar{c}$.

3.2. Phonon modes related to the RS layers

Vibrational modes localized in the RS layers are expected to exist in $RTaS_3$ compounds as in the $RNbS_3$ compounds [9]. According to the group-theoretical analysis based on the approximate layer symmetry of D_{4h} for the RS layer [9], two A_{1g} modes of the RS layer are predicted in the present experimental geometry. The displacements of atoms for the two A_{1g} modes are depicted schematically in figure 4. In one of these modes, the R and S atoms in the same plane move out of phase along the c axis (figure 4(a)) and in the other mode they vibrate in phase along the c axis (figure 4(b)). If the stretching force constant between the nearest R and S atoms in the different planes dominates over the bending force constant for S–R–S in the same plane, the frequency of the out-of-phase motion (the lower-frequency mode) would depend on the total mass $M_R + M_S$, where M_R and M_S are the masses of R and S atoms, respectively, whereas the frequency of the in-phase motion (the upper-frequency mode) would depend on the reduced mass $\mu_R = M_R M_S/(M_R + M_S)$. The lower-frequency and higher-frequency modes are designated as RS1 and RS2 modes, respectively, hereafter. In fact, the bending force constant for S–R–S in the same plane is not negligibly small, and hence two modes may mix since they belong to the same irreducible representation.

The two Raman bands observed in the frequency region from 100 to 200 cm^{-1} shown in figures 1 and 2 are assigned to the intralayer vibrational modes of the RS layer following the previous analysis of $RNbS_3$ (R ≡ La or Ce) [6]. These modes are the out-of-plane vibrational modes.

First, we discuss the dependence of the frequencies of the RS1 and RS2 modes on the mass of the rare-earth atoms. The RS1 band frequency shifts downwards from about 122 cm^{-1} (R ≡ La) to about 116 cm^{-1} (R ≡ Gd) as M_R increases. The frequency ratio of the LaS and GdS modes coincides with the calculated ratio $\sqrt{(M_{Gd} + M_S)/(M_{La} + M_S)} = 1.05$. On the other hand, the frequency of the RS2 band is almost independent of R atoms within experimental error. This observation agrees with our expectation that the frequency of the

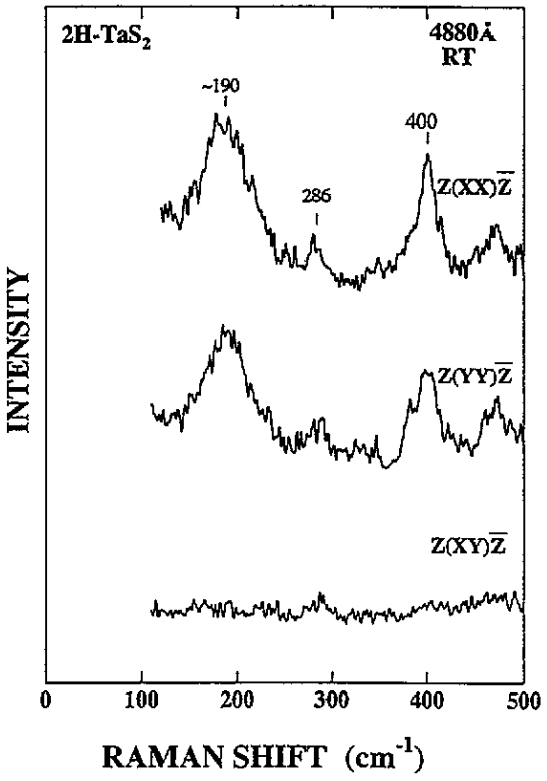

Figure 3. Polarized Raman spectra of 2H-TaS_2 measured at room temperature: (*a*) $Z(XX)\bar{Z}$, (*b*) $Z(YY)\bar{Z}$ and (*c*) $Z(XY)\bar{Z}$, where X and Y refer to the directions which are orthogonal to each other in the basal plane, and Z refers to the direction perpendicular to the basal plane.

Table 1. Observed peak frequencies of the Raman-active phonons of $LaTaS_3$, $CeTaS_3$, $SmTaS_3$, $GdTaS_3$, 2H-TaS_2 and $(EDA)_{0.3}TaS_2$.

	Peak frequency (cm^{-1})					
Mode	$LaTaS_3$	$CeTaS_3$	$SmTaS_3$	$GdTaS_3$	2H-TaS_2	$(EDA)_{0.3}TaS_2$
A	122	126	118	116	—	—
A	148	146	150	149	—	—
Two-phonon	255	258	—	267	190	200
	293	296	297	294	—	—
E	324	324	324	330	286	300
A	399	401	398	398	400	395

RS2 band is proportional to the square root of the reduced mass μ_R and that the values of μ_R for the LaS and GdS layers are almost the same. These analyses indicate that the frequency change of the RS1 and RS2 modes with the rare-earth species is caused by the mass change of the R atoms.

The frequencies of the RS modes of $RTaS_3$ are considerably different from those of $RNbS_3$ (R ≡ La or Ce) [6]. For example, the peaks of $LaTaS_3$ are observed at about 122 and 148 cm^{-1} whereas those of $LaNbS_3$ are observed at about 139 and 200 cm^{-1}. This observation shows that the frequencies of the RS modes depend strikingly on the metal

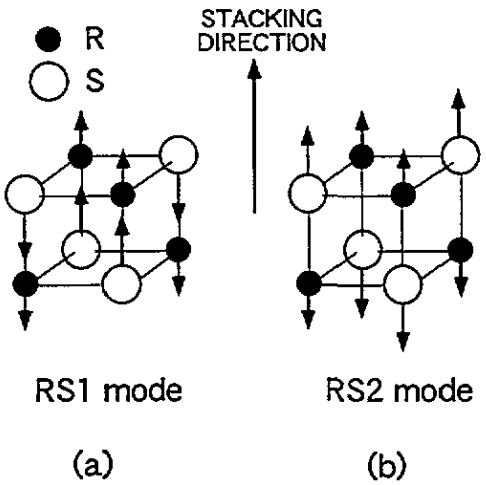

Figure 4. Schematic displacements of atoms for two A_{1g} modes in the RS layer.

species of the TS_2 layer (T ≡ Nb or Ta). In contrast with the Raman spectral features in $RTaS_3$ and $RNbS_3$, the frequencies of the Raman bands relevant to the vibration of the PbS layers in $PbTiS_3$ and $PbNbS_3$ are nearly the same in spite of the considerable difference between the atomic masses of Ti and Nb [9]. In this case, the amount of CT is small and the interlayer interaction is weak. The observed dependence of the RS mode frequency on the T ion in RTS_3 (R ≡ rare earth element; T ≡ Nb or Ta) indicates that firstly the interlayer interactions in RTS_3 are relatively strong and/or secondly there is a difference between the amounts of CT for $RTaS_3$ and $RNbS_3$.

Relatively strong interlayer interactions might bring about the mixing of the intralayer RS and Ta(or Nb)S_2 vibrational modes. However, the observed dependence of the RS modes on R atoms shows that the displacement of Ta atoms in the TaS_2 layers contributes little to the RS mode. Therefore, it is unlikely that we can interpret the frequency difference between the RS modes of $RTaS_3$ and $RNbS_3$ in terms of the mixing only. The CT would increase the intralayer interaction as well as the interlayer interaction. The CT affects the valency of the R ion in the RS layer and reinforces the ionic bonding between the R and S atoms. This results in an increase in the frequencies of the RS modes. The fact that the frequencies of the LaS modes in $LaNbS_3$ are higher than those of $LaTaS_3$ suggests that the amount of CT is larger for $LaNbS_3$ than for $LaTaS_3$.

Alternation in the intensity occurs between the RS1 and RS2 modes (the bands at about 120 and about 150 cm^{-1} in figure 1) on changing the rare-earth elements. The intensity ratio of the RS1 band to the RS2 band becomes large when La is replaced by heavier rare-earth elements. As seen in figure 4, the modulation amplitude of the R–S bond length (R–S bond between different planes) is larger for the RS2 mode than for the RS1 mode. According to the bond polarizability model [13], in which the Raman tensors are associated with the change in the Raman bond polarizability by the vibrational displacements of the constituent atoms, the RS2 mode is expected to give a larger Raman tensor than the RS1 mode irrespective of the species of the R atom. This is in contrast with the present experimental result. Therefore, it seems difficult to explain the intensity alternation within the framework of the bond polarizability model. The effect of the CT and also the difference between the stacking structures of La(Ce)TaS_3 and Sm(Gd)TaS_3 mentioned in section 3.1 should be taken into account to explain the experimental result.

3.3. Phonon modes related to the TaS_2 layers

For the vibration of the TaS_2 layer, one A_{1g} mode and one E_{2g} mode (irreducible representations for the D_{6h} symmetry of 2H-TaS_2 are used for simplicity) are expected to be observed under the back-scattering geometry.

A narrow band at about 325 cm^{-1} appears for any polarization geometry as shown in figure 2. For $GdTaS_3$, the corresponding band is located at 330 cm^{-1}. This band has the same polarization property as the E^1_{2g} mode of 2H-TaS_2 (286 cm^{-1}). We therefore attribute this band to the intralayer E mode of the TaS_2 layer. It is to be noted that the E mode upshifts by about 40 cm^{-1} from the peak frequency of the E^1_{2g} mode of 2H-TaS_2 (see table 1). The band observed at about 400 cm^{-1} shows the same polarization property as the A_{1g} mode of 2H-TaS_2 and the peak frequency of $RTaS_3$ is nearly the same as that of 2H-TaS_2 (400 cm^{-1}). Therefore, it is assigned to the intralayer A mode of the TaS_2 layer, which corresponds to the A_{1g} mode in 2H-TaS_2. In contrast with the E mode, the frequency of this band is nearly the same as in the A_{1g} mode of 2H-TaS_2 and is independent of rare-earth species.

From table 1, the E modes of the TaS_2 layer of $RTaS_3$ upshift by about 40 cm^{-1} with respect to that of 2H-TaS_2. The amount of upshift is comparable with that observed for $RNbS_3$ (R $\equiv$ La or Ce), in which the large amount of the CT (0.7 electrons/Nb or more) occurs [6]. This upshift is considerably larger than that observed in EDA-intercalated TaS_2 (14 cm^{-1}) [8], $SnNbS_3$ and $PbNbS_3$ (about 30 cm^{-1}) [9], where the CT is estimated to be less than 0.2 electrons/Nb. This upshift in the E mode has been interpreted as being induced by the CT [14] and the upshift in the E mode for $RTaS_3$ and $RNbS_3$ indicates that a comparable CT occurs in these compounds. The large amount of CT for $RTaS_3$ is consistent with the results of the optical reflectance and Hall measurements [2]. However, the intralayer A mode of $RTaS_3$ remains at nearly the same frequency as that of 2H-TaS_2 although it shifts upwards by about 15 cm^{-1} for $RNbS_3$ (R $\equiv$ La or Ce). This result suggests that the amount of CT in $RTaS_3$ is less than that in $RNbS_3$.

For $RTaS_3$ the relative intensity of the E mode with respect to the A mode relevant to the TaS_2 layer is considerably different from that of 2H-TaS_2. The relative intensity ratio of the E mode with respect to the A mode is considerably stronger for $RTaS_3$ than for 2H-TaS_2. This means that the Raman intensity and the frequency are affected by the CT.

3.4. Extra modes

Figure 5 shows polarized Raman spectra of $LaTaS_3$ in the frequency region 330–480 cm^{-1}. A band centred at 357 cm^{-1} is observed strongly in the $c(bb)\bar{c}$ geometry and is weaker or disappears in the $c(aa)\bar{c}$ or $c(ab)\bar{c}$ scattering geometry. Another band appears at 365 cm^{-1} in the $c(aa)\bar{c}$ and $c(bb)\bar{c}$ scattering geometries (in the latter geometry, the 365 cm^{-1} band is seen as a shoulder of the strong 357 cm^{-1} band). This band disappears in the $c(ab)\bar{c}$ scattering geometry. These bands are not understood in terms of the intralayer vibration of the isolated TaS_2 and LaS layers and therefore we refer to these bands as 'extra bands'. The extra bands are observed at around 360–370 cm^{-1} for other misfit layer compounds studied in this work. Such extra bands are also observed for $RNbS_3$ [6, 14]. The extra bands are very weak for $SmTaS_3$ and $GdTaS_3$ in figures 1 and 2 and could be observed when a highly sensitive CCD detector was used. The Raman profiles are different for $c(aa)\bar{c}$ and $c(bb)\bar{c}$ geometries as shown in figure 5, indicating that extra bands are anisotropic in the a–b plane. The b axes of the TaS_2 and the RS layers are commensurate with each other whereas the a axes are incommensurate. Thus the stress on the TaS_2 layer might be anisotropic. The appearance of these bands indicates that the interlayer interaction between the RS layer and

the TaS_2 layer is relatively strong. The strong interlayer interaction arising from the CT may cause the breakdown of the pseudo-hexagonal symmetry of the TaS_2 layer and hence may induce the difference between the spectra for two geometries $c(aa)\bar{c}$ and $c(bb)\bar{c}$. On the contrary, according to Suzuki *et al* [2], the optical reflection spectra for $E \parallel a$ are similar to those for $E \parallel b$ in the energy region between 750 and 25 000 cm^{-1}. This means that the electronic structure, which is dominated by the d_{z^2} conduction band of the TaS_2 layer, is isotropic in the a–b plane and may not be significantly changed by the incommensurate positional modulation of the sulphur atoms in the TaS_2 layer. However, the anisotropic vibrational spectra demonstrate the anisotropic nature of interlayer bonding.

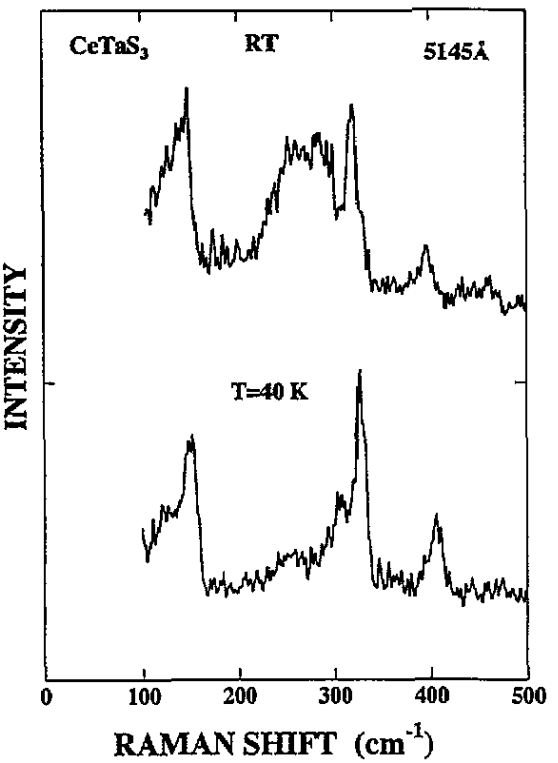

Figure 5. Polarized Raman spectra of $LaTaS_3$ in the frequency range 330–480 cm^{-1} measured at room temperature.

3.5. Electronic Raman bands in $CeTaS_3$

We measured the Raman spectra of $CeTaS_3$ in the high-frequency region at 20 K in order to obtain direct information on the valency of the Ce ions. If Ce ions exist as a trivalent state in a crystal, they have one electron in the 4f orbital. At low temperatures, it is expected that the electronic Raman bands corresponding to the $^2F_{5/2} \rightarrow {}^2F_{7/2}$ transition multiplets in Ce^{3+} are detected at around 2200 cm^{-1} [15]. Although a highly sensitive CCD detector was used, electronic Raman bands could not be found for $CeTaS_3$ with an intensity of at least more than a tenth of the E mode (about 324 cm^{-1}). This electronic Raman band has not been observed in the Raman spectra of $CeNbS_3$ either [14]. These results may be

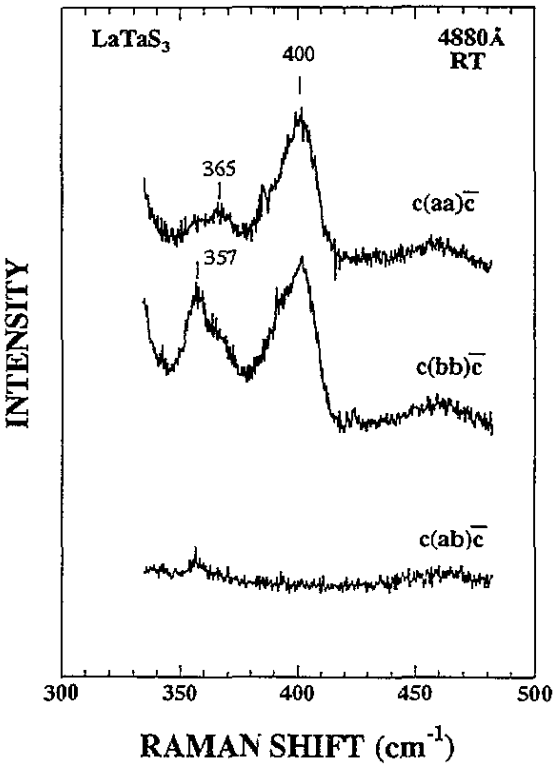

Figure 6. Unpolarized Raman spectra of $CeTaS_3$ measured at (*a*) room temperature and (*b*) 40 K.

attributed to the fact that there are many inequivalent Ce ions with different crystal fields because of the incommensurate structure in the misfit layer compounds, which smears out the electronic Raman band.

3.6. Two-phonon scattering and Kohn anomaly

Broad bands are observed between 200 and 300 cm^{-1} for $RTaS_3$ as shown in figure 1. These broad bands have the same polarization properties as the two-phonon band of 2H-TaS_3 (see figures 2 and 3). Unpolarized Raman spectra of $CeTaS_3$ taken at room temperature and 40 K are shown in figure 6. On cooling the sample from room temperature to 40 K both E and A modes shift upwards by 6–10 cm^{-1}. The intensity of the broad band becomes very weak at the lower temperature (40 K) relative to those of the E and A modes. These results suggest that the broad bands observed between 200 and 300 cm^{-1} are the two-phonon bands. It is worth mentioning that these broad bands have complex structures (peaks at about 260 and about 295 cm^{-1}) and the frequency of the lower peak is higher by about 70 cm^{-1} than that of 2H-TaS_2. The lower-frequency peak (about 260 cm^{-1}) can be assigned to the two-phonon scattering of the Kohn anomaly mode (acoustic mode). The higher-frequency peak (about 295 cm^{-1}) is approximately twice the frequency of the RS2 mode (about 150 cm^{-1}) of the RS layer. Therefore, there is a possibility that this peak is due to simultaneous generation of the two RS2 phonons of the RS layer. An alternative interpretation is possible for the two peaks of the broad two-phonon band. According to the theoretical calculation of the phonon dispersion for 2H-NbS_2 by taking account of the electron–phonon interaction based

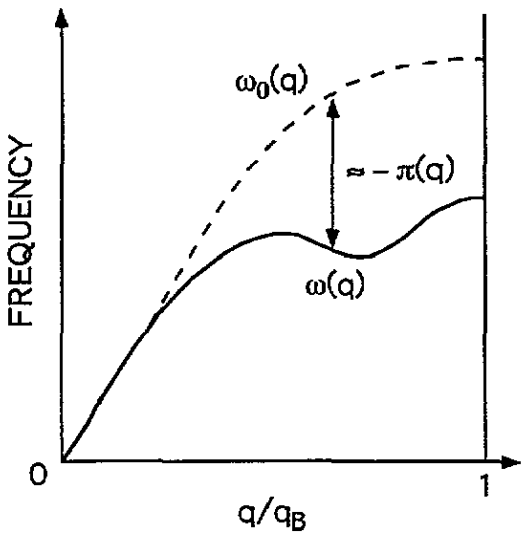

Figure 7. A schematic diagram of the anomalous dispersion curve for the Kohn-anomaly mode (——): – – –, normal dispersion curve neglecting the electron–phonon interaction. q_B indicates the magnitude of the wavevector at the zone edge.

on the tight-binding band calculation by Nishio *et al* [16], there are two acoustic phonon branches which show softening along the ΓM direction in the Brillouin zone (Σ_1 and Σ_2). If the softening of the Σ_1 and Σ_2 branches remains in $RTaS_3$, it is possible to assign the experimental lower and higher peaks to the two-phonon bands of the Kohn anomaly modes of the Σ_1 and Σ_2 branches, respectively.

According to Maldague and Tsang [17] and Klein [18], the intensities of the two-phonon bands in 2H-transition-metal dichalcogenides are proportional to the square $|\pi(q)|^2$ of the phonon self-energy, where q is the wavevector. The magnitude of $\pi(q)$ is enhanced by the nesting of the quasi-two-dimensional Fermi surface for the 2H-polytype transition-metal dichalcogenides. The dispersion of the Kohn anomaly mode is shown schematically in figure 7. The peak frequency of the two-phonon band decreases with increasing $\pi(q)$ because this band corresponds to the simultaneous generation of two Kohn-anomaly acoustic phonon modes having opposite wavevectors and the degree of the softening of this mode increases with increasing $\pi(q)$. The increase in the frequency of the two-phonon band in $RTaS_3$ compared with that of pristine TaS_2 indicates that the magnitude of the phonon self-energy decreases. The variation in the phonon self-energy may be caused by the change in the nesting area and/or the change in the nesting vector. Such changes in the nesting condition might occur by CT from the RS layer to the TaS_2 layer. In contrast with the case of $RTaS_3$, the two-phonon bands in $RNbS_3$ disappear almost completely [14]. This means that the amount of CT for $RTaS_3$ is less than that for $RNbS_3$ and/or that the influences of the CT on the nesting are different for the two compounds because of the difference between the structures of their conduction bands.

The change in the nesting condition may prevent the CDW transition. The strong interlayer interaction between the RS layer and the TaS_2 layer results in the incommensurate potential for electrons in the TaS_2 layer. This incommensurate potential competes with the CDW formation and also contributes to preventing the CDW transition in $RTaS_3$. We consider that the absence of the CDW transition in $RTaS_3$ is due to the above two reasons.

4. Summary

Polarized Raman scattering experiments have been carried out on the misfit layer compounds $RTaS_3$ (R ≡ La, Ce, Sm or Gd) at room temperature and 40 K. The Raman spectra of all compounds are similar to each other because they have essentially the same crystal structure. The mode assignments have been made by comparison with the Raman spectra of 2H-TaS_2 and $RNbS_3$. In contrast with the A mode, the intralayer E mode of the TaS_2 layer upshifts by about 40 cm^{-1} relative to the E^1_{2g} mode of 2H-TaS_2. Extra modes, which cannot be assigned to the intralayer vibrations, are observed. These results are interpreted in terms of the large amount of CT and the resulting increase in intralayer and interlayer interactions. The strong two-phonon bands are observed in $RTaS_3$, the frequencies of which shift towards a higher energy relative to that of 2H-TaS_2. This result can also be understood by the change in the nesting condition of the Fermi surface caused by the CT from the RS layer to the TaS_2 layer. Comparison of the first- and second-order phonon Raman spectra of $RTaS_3$ and $RNbS_3$ indicates that the amount of CT is less for $RTaS_3$ than for $RNbS_3$.

References

[1] Suzuki K, Kondo T, Enoki T and Bandow S 1993 *Synth. Met.* **55–7** 1741
[2] Suzuki K, Kondo T, Enoki T and Tajima H 1994 *Mol. Cryst. Liquid Cryst.* **245** 43
[3] Suzuki K, Kojima N, Ban T and Tsujikawa I 1990 *J. Phys. Soc. Japan* **59** 266
[4] Suzuki K, Enoki T and Bandow S 1993 *Phys. Rev.* B **48** 11 077
[5] Wiegers G A, Meetsma A, Haange R J and de Boer J L 1991 *J. Less-Common Met.* **163** 347
[6] Hangyo M, Nishio T, Nakashima S, Ohno Y, Terashima T and Kojima N 1993 *Japan. J. Appl. Phys. Suppl.* **32** 581
[7] Sugai S 1985 *Phys. Status Solidi* b **129** 13
[8] Hangyo M, Nakashima S and Mitsuishi A 1983 *Ferroelectrics* **52** 151
[9] Hangyo M, Nakashima S, Hamada Y, Nishio T and Ohno Y 1993 *Phys. Rev.* B **48** 11 291
[10] Weigers G A and Meerschaut A 1992 Misfit layer compounds $(MS)_nTS_2$ (M = Sn, Pb, Bi, rare earth metals; T = Nb, Ti, V, Cr; $1.08 < n < 1.23$): structures and physical properties *Incommensurate Sandwiched Layered Compounds* ed A Meerschaut (Aedermannsdorf: Trans Tech) pp 101–72
[11] Sugai S, Murase K, Uchida S and Tanaka S 1981 *Solid State Commun.* **40** 399
[12] McMullan W G and Irwin J C 1984 *Can. J. Phys.* **62** 789
[13] Nakashima S, Katahama H, Nakakura Y and Mitsuishi A 1986 *Phys. Rev.* B **33** 5721
[14] Hangyo M, Kisoda K, Nishio T, Nakashima S, Terashima T and Kojima N 1994 *Phys. Rev.* B **50** 12 033
[15] Mörke I, Kaldis E and Wachter P 1986 *Phys. Rev.* B **33** 3392
[16] Nishio Y, Shirai M, Suzuki N and Motizuki K 1994 *J. Phys. Soc. Japan* **63** 156
[17] Maldague P F and Tsang J C 1977 *Proc. Int. Conf. on Lattice Dynamics* ed M Balkanski (Paris: Flammarion Sciences) p 602
[18] Klein M V 1981 *Phys. Rev.* B **24** 4208